Earthquake Engineering, Tenth World Conference © 1992 Balkema, Rotterdam. ISBN 90 5410 060 5

Ground motion simulation by using simplified three-dimensional finite element method

T.Toshinawa & T.Ohmachi
Tokyo Institute of Technology, Japan

ABSTRACT : A simplified three-dimensional finite element method was applied to Love wave propagation in three-dimensional sedimentary basins. The southern part of the Kanto plain of about 2,000km^2 area was three-dimensionally modeled by the use of the method. Time histories of the Near Izu-Ohshima earthquake of 1990 were calculated and compared with observation. Calculated displacement snapshots showed the effect of three-dimensional topography on direction of Love wave propagation.

1 INTRODUCTION

It has been suggested that ground motions with predominant periods ranging from 2 to 10 sec observed on thick sedimentary basins such as Mexico City and Tokyo are due to surface waves generated and amplified in the basins. In and around such cities, large scale structures such as skyscrapers and long span bridges with longer vibrational periods have lately proliferated and ground motions due to surface wave propagation have become significant from an earthquake engineering point of view. Thus, numerical investigations based on two-dimensional models have been conducted to clarify the generation and propagation characteristics of such waves by several investigators in the last two decades(e.g., Trifunac, 1971; Bard and Bouchon, 1985; Vidale and Helmberger, 1988).

In the meantime, during the Near Izu-Ohshima earthquake of 20 February 1990, the epicenter of which was located 70km south of the Kanto plain, the observed Love waves with the predominant period about 8 sec seemed to be propagated not from the epicenter but from the southwest(Kinoshita and Fujiwara). Propagation direction was probably affected by irregular interfaces between bedrock and sedimentary layers located at the western end of the Kanto plain(see figure 3). When surface waves are changed their propagation directions, scattering and focussing might be occurred in some districts. In such cases, three-dimensional numerical modeling is required to predict ground motion properly.

In recent years, the effects of three-dimensional topography on ground motions have been numerically investigated since great progress has been made in computers. Sánchez Sesma et al., (1989) investigated the response of a semispherical alluvial valley under incidence of plane SH waves in both frequency and time domains by the boundary method. According to their three-dimensional calculations, spectral amplification and predominant frequency increase significantly in comparison with one-dimensional calculations. Horike et al., (1990) and Ohori et al., (1990a) extended the Aki and Larner method (Aki and Larner, 1970) in two dimensions to three dimensions, and applied it to the seismic response analysis of simple sediment-filled valleys. In their three-dimensional analyses, amplification and elongation of duration time were obvious in comparison with the associated two-dimensional ones.

However, little investigation using realistic three-dimensional models and earthquake events has been made because of numerical intractability. From these points of view, the authors developed a simplified three-dimensional finite element method by which the degrees of freedom of an analytical model can be reduced(Toshinawa and Ohmachi,1990a; Toshinawa and Ohmachi,1990b). This paper deals with a three-dimensional modeling of Love wave propagation through the southern part of the Kanto plain, Japan.

2 APPLICATION METHOD

The finite element used herein is a prismatic shaped type that is triangular in the horizontal plane as shown in Figure 1. u, v and w are displacements in the directions of x, y and z, respectively. Local nodes 1, 2 and 3 are on the surface, and the other nodes 4, 5 and 6 are below. Displacement in an element in each direction is represented by the product of the nodal displacements and interpolation functions. Using appropriate functions, we can avoid subdivision of sedimentary basins or alluvial deposits into sublayers so that large three-dimensional areas can be modeled by the present method.

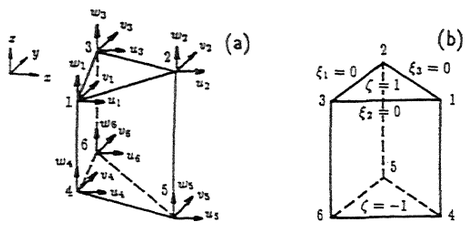

Figure 1. A finite element used in the scheme. (a) in global Cartesian co-ordinates (b) in local co-ordinates

The prismatic element in global Cartesian coordinates in Figure 1a can be simply expressed by local coordinates shown in Figure 1b. In terms of the local coordinates and interpolation functions, displacements in the elements are expressed as follows;

$$u = \sum_{i=1}^{6} N_i u_i, \quad v = \sum_{i=1}^{6} N_{i+6} v_i, \quad w = \sum_{i=1}^{6} N_{i+12} w_i \tag{1}$$

where,

$$N_{6(k-1)+j} = \xi_j f_k(\zeta), \quad N_{6(k-1)+j+3} = \xi_j \{1 - f_k(\zeta)\}$$
$$(j = 1,2,3; \quad k = 1,2,3) \tag{2}$$

$f_1(\zeta)$, $f_2(\zeta)$, and $f_3(\zeta)$ are the interpolation functions for u, v and w along the z axis, respectively. These functions are determined from eigenfunctions for the fundamental-mode surface waves(Toshinawa and Ohmachi, 1990). As an example, interpolation functions $f_1(\zeta)$, $f_2(\zeta)$, and $f_3(\zeta)$ for Poisson's ratio 0.40 are illustrated in Figure 2. When displacements in the element are expressed by the values at the nodes, stiffness and mass matrices can be evaluated. Toshinawa and Ohmachi (1990a) gives details of how these matrices have been evaluated.

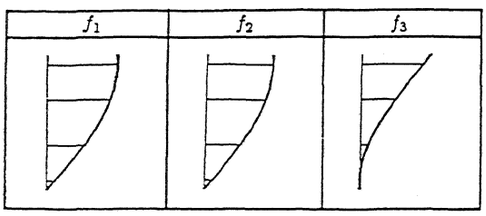

Figure 2. Shape functions used in the scheme. The functions represent displacement distribution in an element for Poisson's ratio 0.40.

In wave propagation analyses, one of the difficulties in using finite element procedure is contamination of the solution due to reflections from fictitious boundaries. To overcome this difficulty, viscous dampers (Lysmer and Kuhlemeyer, 1969) are applied to the boundaries. If the vertical plane constituted by the nodes 1, 3, 4 and 6 in Figure 1a is a laterally fictitious boundary, damping matrix for the element is expressed as follows;

$$\mathbf{c}_s = \begin{bmatrix} \mathbf{c}_1 & & & & & \\ & 0 & & & 0 & \\ & & \mathbf{c}_1 & & & \\ & & & \mathbf{c}_1 & & \\ & 0 & & & 0 & \\ & & & & & \mathbf{c}_1 \end{bmatrix} \tag{9}$$

where,

$$\mathbf{c}_1 = \frac{\rho A_s}{4} \begin{bmatrix} V_X & 0 & 0 \\ 0 & V_Y & 0 \\ 0 & 0 & V_s \end{bmatrix}$$

in which $V_{X(Y)} = V_s \cos\theta_{X(Y)} + V_p \sin\theta_{X(Y)}$. V_p and V_s are velocities of compressional and shear waves. $\theta_{X(Y)}$ is the angle between the boundary and the plane $y = 0$ ($x = 0$), and A_s is the area of the side boundary.

As for the basement boundary, when the basement plane constituted by the nodes 4, 5 and 6 in Figure 1a is underlain by an elastic basement, the corresponding damping matrix can be evaluated as follows;

$$\mathbf{c}_b = \begin{bmatrix} 0 & & 0 & \\ & \mathbf{c}_2 & & \\ 0 & & \mathbf{c}_2 & \\ & & & \mathbf{c}_2 \end{bmatrix} \tag{10}$$

where,

$$\mathbf{c}_2 = \frac{\rho_b A_b}{3} \begin{bmatrix} V_x & 0 & 0 \\ 0 & V_y & 0 \\ 0 & 0 & V_z \end{bmatrix}$$

in which $V_{x(y,z)} = V_{sb} \cos\theta_{x(y,z)} + V_{pb} \sin\theta_{x(y,z)}$, $\theta_{x(y,z)}$ is the angle between the basement and the x-(y-, or z-) axis. A_b is the area of the basement boundary, ρ_b, V_{pb} and V_{sb} are the mass density, compressional and shear wave velocities of the basement, respectively.

Finally, the damping matrix c can be evaluated by

$$\mathbf{c} = \mathbf{c}_s + \mathbf{c}_b + a_0 \mathbf{m} + a_1 \mathbf{k} \tag{11}$$

where a_0 and a_1 are the factors for the Rayleigh damping.

With element matrices m, k, and c, matrices for an entire system can be readily constructed by superposing them appropriately. More details in numerical techniques are given in (Toshinawa and Ohmachi,1990b).

3 NUMERICAL MODELING

Many explosion tests have been conducted in the southern part of the Kanto plain, Japan and two-dimensional underground structures have been obtained by several researchers (e.g. Yamanaka et al.,1986). Strong ground motion observations are also

conducted in the area. During the 1990 Near Izu-Ohshima earthquake, strong ground motions were obtained at the stations shown by the filled circles in Figure 3.

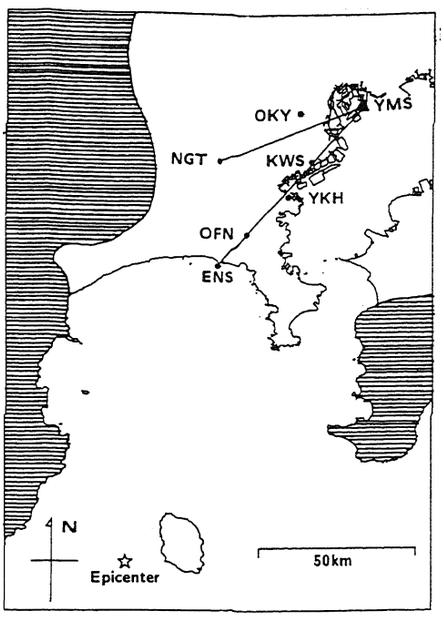

Figure 3. Map of the southern part of the Kanto plain, Japan. Cross-hatched areas show surface exposure of the bedrock.

According to the observation, horizontal motions of about 8 sec period were predominant, even though vertical motion of shorter period is perceptible at a few stations. The horizontal motion of about 8 sec period has often been observed in earthquake recordings from this area, and is attributed to Love waves(Yamanaka et al., 1991b).

To perform wave propagation analysis by the use of the present method, three-dimensional modeling of the southern part of the Kanto plain was conducted as shown in Figure 4a. Although the subsurface ground is multi-layered soil and has a velocity gradient with depth, the ground was idealized as double-layered elastic media for simplicity.

The basement interface is also illustrated in Figure 4b with vertical exaggeration 2:1. Shear-wave velocity and Poisson's ratio for the surface layer are 1km/s and 0.40, whereas those for the bedrock are 3km/s and 0.25, respectively. Interpolation functions used here are the same as those in Figure 2. Depths to basement were obtained by referring geological data and underground structures evaluated by Yamanaka et al.(1986, 1991a) as are depicted by solid lines in Figure 3. The western part of the model is shallow as the Kanto plain is bounded by exposed bedrock at the western side.

The element size is 0.5km long and 0.5km wide, that makes the longest length between adjacent nodes 0.71 km. As more than eight elements are necessary for any wavelength to secure accuracy of the solution(Kuhlemeyer and Lysmer, 1973), wavelengths to be discussed here are longer than 5km approximately. When seismic waves are propagated in the basin at 1 km/s, the corresponding period becomes 5 sec. The total length and width of the model are 48.5km and 38.5km, with the area of about 2,000km^2. Since the present simulation deals with Love waves, each node is allowed horizontal displacement only. Nevertheless, there are 14,422 nodes and 28,844 degrees of freedom.

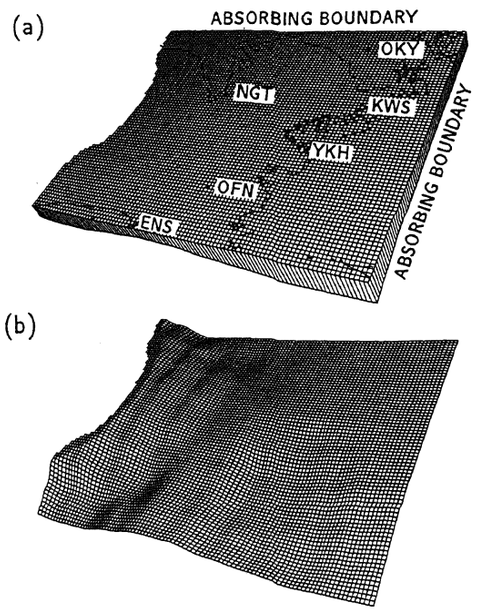

Figure 4. (a) Three-dimensional finite element modeling of the southern part of the Kanto plain, Japan. (b) Basement interface of the model.

The epicenter is located almost south of the model, so velocity waves observed at ENS were input at the south and the southern part of the western boundary, with a slight modification in amplitude and phase lag based on the epicentral distance. Deconvolved time histories based on subsurface structure at ENS were applied at the entire basement surface and the northern part of the western boundary where the bedrock is exposed. The input waves applied at ENS are shown in Figure 5. As the minimum period for the elements in eigenvalue analysis is approximately 0.5 sec, the time interval for the numerical integration is set to 0.05 sec. No damping is considered here as attenuation is roughly negligible at around 10 sec period. The step-by-step integration was performed for 4001 time steps.

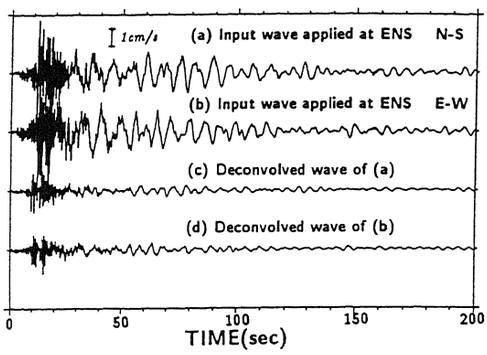

Figure 5. Input waves applied at ENS.

4 NUMERICAL RESULTS

Observed and calculated time histories are compared in Figure 6. All the waveforms are low-pass filtered at 0.2 Hz. Predominant periods and duration times are similar between observations and calculations as a whole. Synthetics at OFN and YKH are satisfactory with respect to amplitude. Meanwhile, calculated amplitude at KWS is smaller than the observation in the north-south direction, but larger than that in the east-west direction. The calculation at OKY has less amplitude in the north-south direction only. The differences between the observation and the calculation might be due to inappropriateness of several factors involved in the calculation such as input bedrock motion, geological ground structure and its numerical modeling.

Horizontal displacement snap shots at all points at every 20 sec interval are presented in Figure 7. Direction of input wave propagation and the initial polarization are depicted in Figure 7a and 7b, respectively. The Love wave propagation is seemingly overall toward the northeast direction before 60 sec, while it becomes localized and complicated after 60 sec. Wave fronts at 20 sec are along initial polarization. At 40 sec, in the meantime, reflected waves are propagated from the western bedrock changing their polarization in the basin. Large amplified waves of about 10km wavelength are propagated from the southeast to the northeast(see figure 7d and 7e). This is because surface waves are amplified in the deep alluvial deposits beneath the southeast district(see figure 4b). Surface waves have almost passed away at 140sec(see figure 7h).

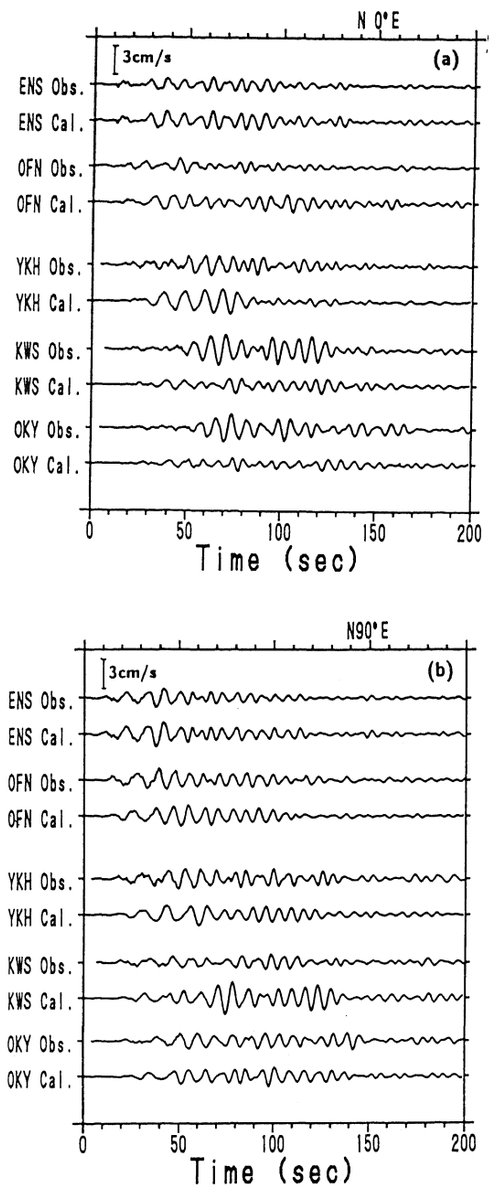

Figure 6. Comparison of time histories between observations and calculations.
(a) N-S component. (b) E-W component.

5 CONCLUSIONS

A simplified three-dimensional finite element method has been developed and applied to the Love wave propagation problem in the southern part of the Kanto plain, Japan during the 1990 Near Izu-Ohshima earthquake. Because of requiring a relatively small number of degrees of freedom, the three-dimensional finite element method presented here was adaptable to analysis on Love wave propagation in an area as large as 2,000 km^2.

As well as strong motion records from the 1990 Near Izu-Ohshima earthquake, calculated polariza-

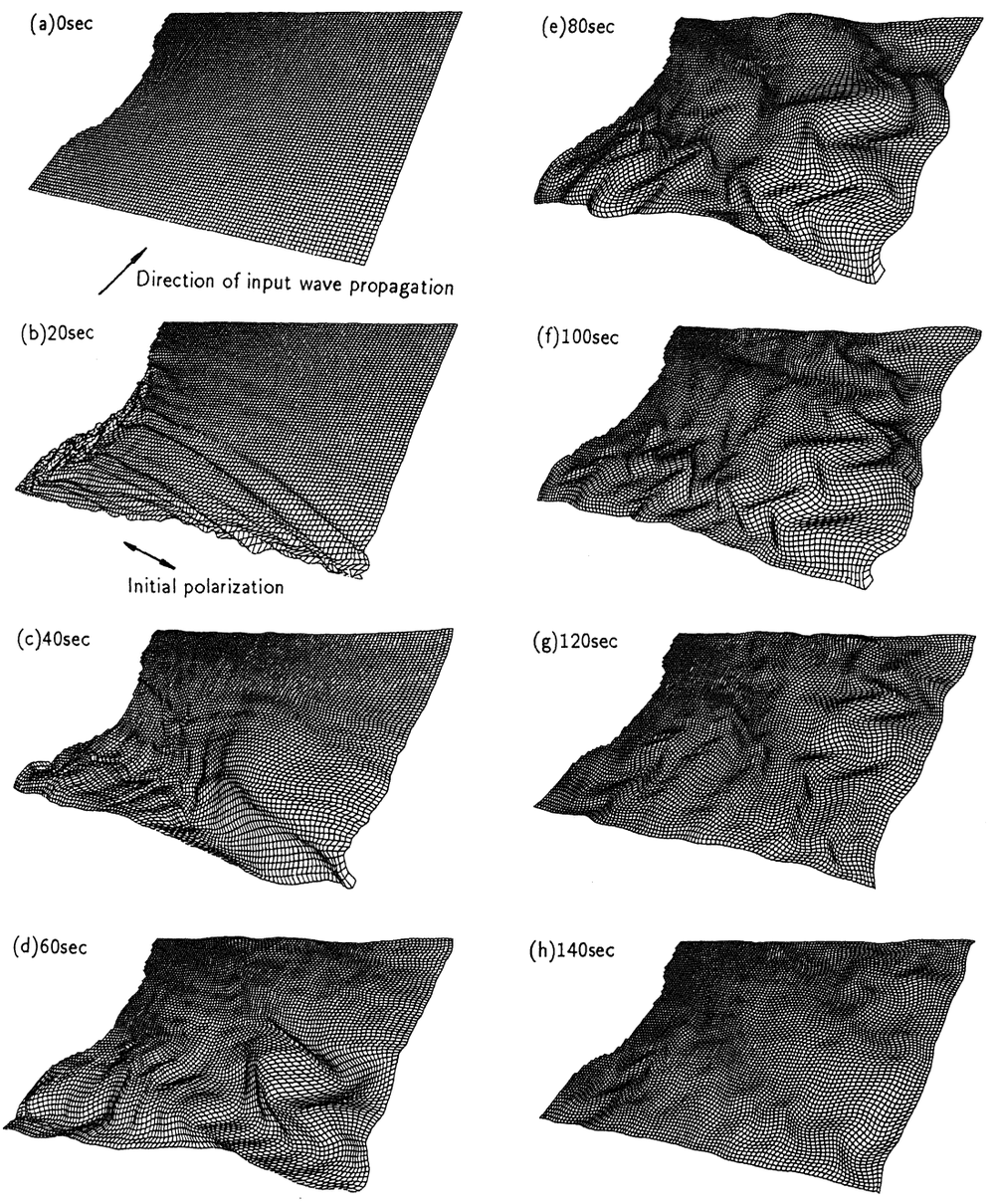

Figure 7. Horizontal displacement snap shots.

tions rotate clockwise in some districts of the basin because of the reflected waves propagated from the west bedrock. The calculation demonstrated that the three-dimensional topography of bedrock had a considerable influence on Love wave propagation. The influence includes amplification in amplitudes, protraction of duration times and rotation of wave paths.

The present method proved to be capable of analyzing Love wave propagation in a large area with irregular basement topography. At present, as the method has been formulated for double-layered media only, it cannot represent effects of locally deposited thin layers.

ACKNOWLEDGMENTS

Thanks are given to Kazuoh Seo and Takanori Samano for offering the strong ground motion records. Useful comments were provided by Saburoh Midorikawa. The numerical computation for this study was performed on the ETA^{10}, and partly supported by Computer Center, Tokyo Institute of Technology.

REFERENCES

Aki, K. and K. Larner (1970). Surface motion of a layered medium having an irregular interface due to incident plane SH waves, *Journal of Geophysical Research*, **75**, 933-954.

Bard, P.-Y. and M. Bouchon (1985). The two-dimensional resonance of sediment-filled valleys, *Bulletin of the Seismological Society of America*, **75**, 519-541.

Horike, M. et al. (1990). Seismic response in three-dimensional sedimentary basin due to plane S wave incidence, *Journal of Physics of the Earth*, **38**, 261-284.

Kinoshita, S. and H. Fujiwara (1990). Secondary Love waves observed by a strong motion array in the Tokyo lowlands, Japan *Journal of Physics of the Earth*,(submitted).

Kuhlemeyer, R. L. and J. Lysmer (1973). Finite element accuracy for wave propagation problems, *Journal of the soil mechanics and foundations division, Proceedings of ASCE*, **99** No. SM5, 421-427.

Lysmer, J. M. and R. L. Kuhlemeyer (1969). Finite dynamic model for infinite media, *Journal of the Engineering Mechanics Division, Proceedings of the American Society of Civil Engineers*, **4**, 859-877.

Ohori, M., K. Koketsu and T. Minami (1990a). Seismic response analyses of sediment-filled valley due to incident plane waves by three-dimensional Aki-Larner method, *Bulletin of Earthquake Research Institute*, **65**, 433-461 (in Japanese).

Sánchez-Sesma, F. J., L. E. Pérez-Rocha and S. Chávez-Pérez (1989). Diffraction of elastic waves by three-dimensional surface irregularities. PART II, *Bulletin of the Seismological Society of America*, **79**, 101-112.

Toshinawa, T. and T. Ohmachi (1990a). A simplified 3-D finite element method applied to modal analyses of an elastic surface layer, *Structural Engineering/ Earthquake Engineering*, **7**, 323-330.

Toshinawa, T. and T. Ohmachi (1990b). Impulsive response of a surface layer analyzed by 3-D finite element methods, *Proceedings of the 8th Japan Earthquake Engineering Symposium*, 349-354.

Trifunac, M. D. (1971). Surface motion of a semi-cylindrical alluvial valley for incident plane SH waves, *Bulletin of the Seismological Society of America*, **61**, 1755-1770.

Vidale, J. E. and D. V. Helmberger (1988). Elastic finite-difference modeling of the 1971 San Fernando, California earthquake, *Bulletin of the Seismological Society of America*, **78**, 122-141.

Yamanaka, H., K. Seo, T. Samano and S. Midorikawa (1986). On the seismic prospecting in the southwestern part of the Tokyo metropolitan area(2), *Bulletin of Seismological Society of Japan* **39**, 607-620 (in Japanese).

Yamanaka, H., K. Seo and T. Samano (1991a). On the seismic prospecting in the southwestern part of the Tokyo metropolitan area(4), *Bulletin of Seismological Society of Japan*, **44**, 9-20 (in Japanese).

Yamanaka, H., K. Seo and T. Samano (1991b). Analysis and modeling of long-period ground motion in the Kanto plain, Japan, *Proceedings of the Fourth International Conference on Seismic Zonation*, **2**, 75-82.